ACCRETION–DISK PRECESSION

AND SUBSTELLAR SECONDARIES

IN CATACLYSMIC VARIABLES

JOSEPH PATTERSON
Department of Astronomy, Columbia University
550 West 120th Street, New York, NY 10027
jop@astro.columbia.edu

submitted • *Publications of the Astronomical Society of the Pacific* • 2000 December 29

2001 February 26 Revision

ABSTRACT

The mass-losing secondaries in cataclysmic binaries are progressively whittled away by the ongoing loss of angular momentum. The expected *rate* of evolution implies that the binaries should spend most of their lives at very short orbital period, with light secondaries (<0.08 $M_{\odot}$). But compared to the nearby white dwarf and accretion disk, these secondaries are effectively dark; so it has been quite difficult to learn anything about them from observation. Here we show that for dwarf novae, the majority species, the mass ratios can be measured from simple photometric observations of "superhumps", using equipment commonly possessed by amateur astronomers. The technique basically involves measuring the apsidal precession rate of the accretion disk, and thus has the merit of being purely dynamical, requiring no actual detection of light from the secondary. The results reaffirm what we have known for a long time — that most secondaries are near the main sequence — but also show that near the end of the main sequence at 0.08 $M_{\odot}$, the secondaries are significantly larger. This bloating, possibly due to an extra angular momentum sink in the binary, sets the value of the minimum orbital period for H-rich binaries to be 76–80 minutes. Seven stars are found with secondaries in the mass range 0.014–0.06 $M_{\odot}$.

Subject headings: accretion, accretion disks — binaries: close — novae, cataclysmic variables

1. INTRODUCTION

The great breakthrough in understanding the evolution of cataclysmic variable stars occurred twenty years ago, when it was realized that the main force driving binary evolution is angular momentum loss, probably from gravitational radiation and/or some kind of magnetic wind (Paczynski 1981; Paczynski & Sienkiewicz 1981, 1983; Verbunt & Zwaan 1981; Rappaport, Joss, & Webbink 1982). This finally provided a theoretical method to predict accretion rates. Study of those rates showed that angular momentum loss ($\dot{J}$) must rise sharply with orbital period (Patterson 1984, hereafter P84), and this has led to the popular view that long-period stars are driven mainly by a magnetic wind and short-period stars by gravitational radiation (GR). Today's theories of evolution assume this, and manage to succeed, *mutatis mutandis*, in explaining many features observed in the cataclysmic-variable zoo (Kolb 1993, hereafter K93; Howell, Rappaport, & Politano 1997; Patterson 1998, hereafter P98; Kolb & Baraffe 1999, hereafter KB99; King et al. 1996).

But great puzzles still afflict our understanding of the latest stages of evolution. The most evolved secondaries will be stripped to ~0.08 $M_\odot$ in only 1–4 Gyr, so the Galaxy should be old enough to have produced many binaries with even lighter secondaries. Assuming only GR as a $\dot{J}$ sink, K93 estimated that 70% of all CVs should have such "substellar" secondaries; P98 suggested that some residual magnetic wind, arguably needed to understand other features in the zoo, will speed evolution and therefore only raise this percentage.

Do these substellar secondaries really exist? The answer is almost certainly yes; the observed and theoretical timescales demand it. Perhaps the more interesting question is, do these remnants of CV evolution retain enough of the familiar properties of "cataclysmic variables" to maintain their membership in that class? Or do they mutate into something different, requiring different discovery methods and/or different physics? Unfortunately, the secondaries themselves tend to be not so helpful, as they emit hardly any light. Nuclear luminosity entitles them to only M_V>+19, too feeble to see in proximity to the white dwarf and accretion disk (each of which has M_V~10–12). No light from any of these stars — substellar-secondary candidates — has ever been convincingly detected. And even if one did manage to rise to a respectable fraction of the binary's light at infrared wavelengths, two other complications loom:

(1) Their atmospheres are irradiated by significant UV radiation from the white dwarf, which will weaken the temperature gradient necessary for absorption features.

(2) Their temperatures and luminosities do not actually reveal the present-day masses, but rather arise from their thermal history (since they are likely shining with heat left over from a more glorious past).

In this paper we demonstrate that it is possible to *weigh* the secondaries, even if it is not possible to *see* them. The reason is that most of these binaries show apsidal precession in their accretion disks, and the precession rate is easily measured and proportional to the mass ratio. The results imply that most known dwarf novae have secondaries on or near the main sequence, but a few are substellar. The observed precession rates also provide good constraints on the mass-radius relation for CV secondaries.

2. APSIDAL PRECESSION OF THE ACCRETION DISK

Dwarf novae in superoutburst always show photometric waves ("superhumps") with a period a few percent longer than P_{orb}. A series of papers in 1988–1992 established the reason for this: an eccentric instability grows at the 3:1 resonance in the disk, and the eccentric disk is forced to precess by the perturbation from the secondary (Whitehurst 1988, Lubow 1991, Hirose & Osaki 1990, Lubow 1992). Recent studies have confirmed this, added new details, successfully explained some of the fine points of the observations, and established the basic origin of the superhump: the extra heating associated with the periodic deformations of disk shape (Lubow 1992; Murray 1996, 2000; Kunze et al. 1997; Simpson & Wood 1998; Wood, Montgomery, & Simpson 2000).

In this theory the superhump period P_{sh} is a simple function of P_{orb} and the precession period P_{prec}:

$$1 / P_{sh} = 1 / P_{orb} - 1 / P_{prec}. \tag{1}$$

P_{sh} and P_{orb} are in principle measurable to good accuracy, and therefore so is the fractional excess $\varepsilon=(P_{sh}-P_{orb})/P_{orb}$. Values of ε for 59 CVs are given by P98. P_{prec} is usually not directly observable, but is related through

$$\varepsilon = P_{orb} / (P_{prec} - P_{orb}). \tag{2}$$

We consider only "apsidal" or "positive" ($\varepsilon>0$) superhumps in this paper.

Now the 3:1 orbital resonance in the disk occurs at $R_{disk}/a\approx0.46$, where a is the binary separation. If $q=M_2/M_1$, the mass ratio of secondary star to white dwarf, then elliptical orbits at this radius will experience a dynamical (but nonresonant) apsidal advance at a rate given by

$$\omega_{dyn} = \omega_{orb} \times [0.37\, q / (1 + q)^{½}] \times (R_{disk} / 0.46\, a)^{2.3}, \tag{3}$$

where we have converted to frequency units and used an approximation to the radial dependence of Murray (2000). Eqs. (2) and (3) imply

$$\varepsilon^{-1} = [0.37\, q /(1 + q)^{½}]^{-1} (R_{disk} / 0.46\, a)^{-2.3} - 1, \tag{4}$$

or $\varepsilon\approx0.35q$ for the relevant range of q (0.04–0.30) and at the resonant radius. So if the simple dynamical precession of one particle at this radius captures the essence of the superhump phenomenon, then we can use Eq. (4) to deduce q from the easily measured ε.

That may seem like boundless optimism, since the disk actually contains $\sim10^{47}$ particles, distributed over a wide range in radius. Yet observations, as well as the hydrodynamic calculations, show precession at one rate, not a range of rates. But not necessarily the rate given by Eq. (3); viscosity in the disk acts to slow the precession, in effect adding an extra (subtractive) term to Eq. (3) (Lubow 1991, Murray 2000).

3. CALIBRATING ε(q)

It is hard to estimate the needed correction to Eqs. (3) and (4). In addition to the obvious worry about the poorly known and poorly understood viscosity, these formulae apply only to nonresonant orbits — yet are most commonly applied to R=(0.43–0.48)a, where the 3:1 resonance occurs. They also neglect the role of finite eccentricity, which affects the dynamical precession rate (Danby 1992). These are excellent subjects for future study of the underlying dynamics of the eccentric disk (e.g. Montgomery 2001). For our purposes and at present, it seems wiser to bypass this and rely instead on an *empirical* calibration of ε(q).

Among superhumping CVs, reliable and fairly accurate measurements of q exist for eight eclipsing binaries, shown in the boxes in Figure 1. Table 1 summarizes the sources of the data. Most of the error boxes are small, because the stars yield much information from eclipses of both the white dwarf and the mass-transfer hot spot. This yields an accurate q from the technique first described by Smak (1979, 1996). The case of WZ Sge warrants special mention, though, because it is critical in anchoring one end of Figure 1, and because the errors are bigger (the inclination is high enough to eclipse the hot spot, but not the white dwarf).

There are ~20 published analyses of q in WZ Sge, mainly because the observed stationarity of the emission lines (K_1<37 km/s, Krzeminski & Kraft 1964) in an eclipsing binary implies an interestingly low q. A flurry of studies in 1978–1983 gave estimates or upper limits generally in the range 0.02–0.10. More recent studies have given slightly higher q (0.13±0.02, Smak 1993; 0.075±0.015, Spruit & Rutten 1998), and these estimates are often cited with approval today. However, the latter estimates are based on reported detections of K_1 (respectively 49±5 and 40±10 km/s) which give a phase of white dwarf motion discrepant from the true phase (known from the eclipses) by 47±10º. The problem inflicted by so large a spurious phase shift is fatal. Until we can obtain a K_1 from direct measures of the white dwarf, or learn how to correct for disk/spot distortions, these measures of K_1 from disk emission should be considered at best an upper limit.

Apart from deciding on K_1, which brutally affects the mass solutions, the many studies of WZ Sge differ mainly in the weight they give to the several available clues (eclipse timing, S-wave amplitude, separation of emission-line peaks). We have sifted among this evidence, added K_1<40 km/s, and decided to adopt q=0.045±0.020.

Returning to Figure 1, it appears that a simple linear fit with

$$\varepsilon = 0.216\ (\pm 0.018)\ q \qquad (5)$$

satisfies the data. This relation is physically reasonable, since zero q should produce no precession. And it suggests that the needed subtractive correction term in Eq. (3) scales with q just as the other term does; in effect, we get the right answer over this range of q by using the dynamical formula (3) and assuming R_{disk}/a=0.37. This result is not surprising, since we know from two lines of evidence that a fairly large disk annulus must participate in the superhump: (1) the large amplitude (~0.3 mag) of the signal; (2) the large eccentricity (e>0.3) needed to satisfy observations of eclipse-timing effects (Hessman et al. 1992, Rolfe et al. 2000) and distortion of spectroscopic line profiles (e.g. Honey et al. 1988). It may be that $\langle R_{disk}/a \rangle$=0.37 effectively expresses the weighting over the participating disk radii.

Also included in Figure 1 and Table 1 are ε and q estimates in five superhumping X-ray binaries. Discussions of these have been given by O'Donoghue & Charles (1996), Haswell et al. (2000), and the references cited in Table 1. These q estimates are much more uncertain and indirect than in the eclipsing CVs, and there are some cycle-count worries afflicting the measured ε as well. For one star, V1405 Aql, there is even uncertainty as to whether the superhump is positive (as required for consideration here) or negative. Hence we indicate the X-ray binaries separately in dashed ovals, and do not include them in fitting ε(q). They are shown primarily to emphasize the general finding that ε is low for low q, consistent with the hypothesis that ε is roughly proportional to q.

Most importantly, however, this relation [Eq. (5)] *enables us to estimate* q *for all 66 CVs with apsidal superhumps and known* P_{orb}. In this paper we will use the (P_{orb}, P_{sh}) data from Table 1 of P98, with 13 additional stars represented in Table 2 of the present paper.

4. MASSES AND RADII OF SECONDARIES

Knowledge of q would provide knowledge of both M_2 and M_1, if we had a single other constraint involving M_1 and M_2. The natural source of such a constraint is radial-velocity studies. Unfortunately this is of only limited help. Although a "K_1" solution exists for nearly every one of these stars, these solutions are known to be contaminated by strong distortions which are periodic with P_{orb} yet not indicative of the stars' actual motions (when the latter are independently known from eclipses; Shafter et al. 1988, Thorstensen et al. 1991). For a few stars there are K_2 solutions (usually from absorption lines in the secondary); these are more reliable but quite scarce, since it is difficult to measure K_2 in the presence of competing light from the disk and white dwarf. The observed K_2 solutions need correction also, since the center-of-light is not coincident with the center-of-mass, and these corrections are not precisely known (Robinson et al. 1986).

Despite the difficulties plaguing solutions for individual stars, analyses of masses in CVs generally — which filter out the worst cases, with large errors, severe line distortion, or unconstrained binary inclination — suggest a fairly consistent average value of M_1. Shafter (1983) found $\langle M_1 \rangle$=0.7±0.1 $M_\odot$, and this estimate has not changed much over the years (0.74±0.04 $M_\odot$, Webbink 1990; 0.69±0.13 $M_\odot$ for the short-P_{orb} stars considered here, Smith & Dhillon 1998). For 51 of our 61 stars, we simply adopt M_1=$\langle M_1 \rangle$=0.7 $M_\odot$. For the remaining 10, we regard the available constraint as of sufficient quality to warrant replacing the default M_1 with the measured value; data for these 10 are collected in Table 3.

Now all secondary stars in CVs fill their Roche lobes, and this imposes a strong constraint on M_2 and R_2:

$$P_{\rm orb}\,[\rm hr] = 8.75\,(M_2 / R_2^3)^{-1/2}, \quad (6)$$

with M_2 and R_2 in solar units (Faulkner, Flannery, & Warner 1972). This yields estimates of M_2 and R_2 for all 61 apsidal superhumpers, shown as the dots in Figure 2. The crosses represent the independent high-precision values found in eclipsing CVs.

Figure 2 demonstrates that CV secondaries obey a fairly well-constrained mass-radius relation. A useful approximation to this, valid over $0.04 < M_2 < 0.36$, is given by

$$R_2 = 0.078 + 0.415\,M_2 + 3.16(M_2)^2 - 5.17(M_2)^3, \quad (7)$$

with M_2 and R_2 in solar units. How does this compare with that of the lower main sequence (for single stars)? The most recent stellar models (Baraffe et al. 1998, hereafter BCAH) yield a ZAMS main-sequence relation shown as the BCAH curve in Figure 2. The curve is extended to lower masses by using the models of Burrows et al. (1993), which substantially agree with those of BCAH in the region of overlap. The CV secondaries are seen to be ~15% larger than the model stars for $M_2 > 0.10\ M_\odot$, and ~30% larger at 0.08 $M_\odot$. Can this be due to error in the adopted $\varepsilon(q)$ or $\langle M_1 \rangle$ in our analysis? Those are plausible guesses, but neither seems to be true, because the (M_2, R_2) values in the eclipsing stars — represented by the crosses — are independent of these assumptions.[1] On the contrary, the close nestling of crosses amid the dots suggests that our $\varepsilon(q)$ and $\langle M_1 \rangle$ are unlikely to be far wrong.

Is it possible that the BCAH mass-radius relation underestimates stellar radii for all stars (not just CV secondaries)? Yes, this is possible. Clemens et al. (1998, hereafter C98) studied a large collection of low-mass stars and derived empirical constraints on masses and radii. A fit to that data gives $R_2/R_\odot = 0.90(M_2/M_\odot)^{0.80}$, yielding radii ~15% larger than BCAH. Beuermann et al. (1999) studied this discrepancy and suggested several possible sources of error in the empirical work, eventually concluding that the BCAH mass-radius relation passed sufficient other tests to be considered reliable. Yet, as seen in Figure 2, the C98 relation fits the CV data excellently for $M_2 > 0.08\ M_\odot$. This is puzzling. We speculate that one of the following is true:

(1) The C98 relation is a realistic description of low-mass stars, and CV secondaries are on the main sequence.

(2) The BCAH relation is a realistic description of low-mass stars, and CV secondaries are systematically 15% larger than single stars of the same mass.

For definiteness we shall assume henceforth that (2) is correct, and will use "main-

[1] The adopted $\varepsilon(q)$ relation depends on the eclipsers, so they are not strictly independent. More correctly, any $\varepsilon(q)$ which moves the points near the BCAH curve would leave all the crosses behind, so all the well-determined values of (M_2, R_2) in eclipsing binaries would be anomalous and unexplained.

sequence" or "ZAMS stars" to mean "BCAH stars at t=10 Gyr". This is an appropriate definition for stars of very low mass, since they require a very long time to contract initially to the main sequence. But in application to CVs, it may in part explain why CVs appear to be slightly larger than ZAMS stars. Actual CVs are more likely to have ages roughly in the range 0.1–3 Gyr, and this could make some difference at the low-M_2 end. (An age of 0.2 Gyr would account for the entire effect, but this seems too little to be characteristic of CVs as a class.)

5. ε VERSUS P_{orb}, A TRACER OF BINARY EVOLUTION

CV evolution can also be illustrated in the $\varepsilon(P_{orb})$ plane, which is useful since these are strict observables which can be measured to high precision. Figure 3 shows the observed distribution. We superpose a theoretical path with the method described in P98,[2] adopting Eq. (5) as the $\varepsilon(q)$ prescription and a KB99 mass-radius law (essentially BCAH with eventual loss of thermal equilibrium driven by $\dot{J} = \dot{J}_{GR}$). This generates the bold curve in Figure 3. It errs in two important respects:

(1) The predicted ε is too large essentially everywhere. This is equivalent to the statement "CV secondaries are slightly larger than ZAMS stars" from Section 4.

(2) The "bullet-head" of the curve is probably too sharp. And it reaches too short a P_{orb}, as discussed many times previously (esp. Paczynski & Sienkiewicz 1983; Nelson, Rappaport, & Joss 1986; P98; KB99).

Can these failures be fixed by mild tinkering with the assumed $\langle M_1 \rangle$ and $\varepsilon(q)$? Probably not. A very large shift in $\langle M_1 \rangle$ to 1.1 $M_\odot$ is needed to solve the first problem, and even that does essentially nothing to fix the second problem. It is very likely that the true culprit is the secondary's mass-radius relation. This is easy to show at the long-P_{orb} end. All the apsidal superhumpers with P_{orb}>0.12 d are fairly luminous stars, with $\langle M_V \rangle < +6$ and hence $\dot{M} > 10^{-9}$ $M_\odot$/yr. Thus the mass-transfer timescale $M_2/\dot{M}_2 \sim 10^8$ yrs. The secondaries have a thermal timescale $\sim 3\times10^7$ yrs (M_2^2/R_2L_2), in solar units, which is equivalent to $\sim 10^9$ yrs $(M_2/0.2\ M_\odot)^{-1.5}$ after applying the BCAH M–R and M–L relations.[3] Therefore the secondaries are out of thermal equilibrium, driven presumably by the high $\dot{J}$ from magnetic braking. To estimate the effect of this, we adopted the M–R relations of BK00 for various values of $\dot{M}$, and calculated their effect on $\varepsilon(P_{orb})$. As can be seen at the upper right of both figures, this moves stars slightly above the ZAMS M_2–R_2 relation in Figure 2, and far below the ZAMS $\varepsilon(P_{orb})$ relation in Figure 3. Since these binaries are known to have high $\dot{M}$, this is very likely the correct explanation.

---

[2] Murray (2000) criticized this calculation because it used a rough approximation [the leading term only in the series better approximated by Eq.(3)] for the theoretical $\varepsilon(q)$. However, the empirical calibration of Figure 1 establishes that for practical purposes the P98 $\varepsilon(q)$ was substantially, though somewhat fortuitously, correct.

[3] Just for the record, the latter can be approximated for M_2<0.3 $M_\odot$ by $L_2=0.42(M_2)^{2.70}$, in solar units.

At shorter period, it is less clear. Conventional wisdom since 1983 professes that magnetic braking shuts off in this regime (P_{orb}<0.1 d), with the binary later evolving by $\dot{J}_{GR}$ only. Abrupt termination of magnetic braking at P_{orb}~3 hr produces a sharp 2–3 hr period gap, and the binary reawakens as a CV at P_{orb}~2 hr dominated by $\dot{J}_{GR}$. However, this is only in rough agreement with Figures 2 and 3. These figures demonstrate that essentially *all* superhumping CVs, even those near P_{orb}=2 hr, appear to have slightly oversized secondaries.[4]

What might make these secondaries oversized? Well, since the culprit in accomplishing this at P_{orb}=3–4 hrs — and then again at 1.3 hrs — appears to be a high $\dot{J}$, that should be considered a leading suspect at other values of P_{orb} also. But GR alone cannot produce this. The GR timescale for $\langle M_1 \rangle = 0.7\ M_\odot$ is

$$t_{GR} = \langle J / \dot{J} \rangle \approx 3.5 \times 10^9 \text{ yrs } (P / 2 \text{ hr})^{8/3} (M_2 / 0.2\ M_\odot)^{-1}, \quad (8)$$

which reduces to 5×10^9 yrs $(P/2 \text{ hr})^{1.4}$ for the M_2–P relation implied by the M_2–R_2 relation found above (Eq. 7). This is too long to affect importantly the secondary's mass-radius relation for P>1.4 hr. GR needs some help, just as it needs some help to explain a minimum P_{orb} of ~76 min. A supplementary mechanism for angular momentum loss would fit both needs. A plausible candidate for this extra $\dot{J}$ is magnetic braking, our old friend. This mechanism must be greatly quenched in low-mass secondaries, but it does not strain credulity to suppose that some of it still lingers. Like their more luminous cousins, these low-mass secondaries are convective and rapidly rotating, the essential requirements for a magnetic wind. While magnetic activity in single stars subsides greatly towards the end of main sequence, it does not die out altogether. Flares and coronal X-ray emission, the more observable signatures of magnetic activity, continue right on through the coolest stars known, including even brown dwarfs (Rutledge et al. 2000, Fleming et al. 2000). Since tidal lock with their companions always forces CV secondaries to rotate very rapidly (~130 km/s), they should all be considered candidates to partake of activity (in this case a magnetic wind) which relies on convection and rotation.

Another possibility is $\dot{J}$ through gravitational (not magnetic) interaction with a circumbinary disk, as discussed recently by Spruit & Taam (2001). This removes angular momentum, speeds evolution, and helps to bloat the secondary — hence has most of the features needed to solve this problem.

Now the general trend of the observed points in Figures 2 and 3 (these are essentially equivalent, with Figure 3 the "observational" version) is actually a pretty good match to the KB99 prediction, aside from a vertical offset. For definiteness we assumed a total $\dot{J}=3\,\dot{J}_{GR}$ and interpolated in Table 2 of KB99 and Figures 2 and 4 of BK00 to calculate the effect on $\varepsilon(P_{orb})$.

[4] Sometimes the word *evolved* is used to denote this. We avoid this, because single-star evolution has trained us to associate this with hydrogen depletion and a high central density. Such conditions certainly do not prevail here. On the contrary, the cause of this departure from the main sequence is excess thermal energy in the star, preventing contraction; thus its analogue in single-star evolution is more like a *pre*-main-sequence star!

This is shown as the light solid curve in Figure 3. The secondaries are slightly larger, yielding a smaller M_2 and hence a smaller ε at a given P_{orb}. This solves problem (a) defined above. It also solves problem (b), because these larger secondaries imply a larger P_{orb}, including a larger *minimum* P_{orb}. The superior agreement of the light solid curve in Figure 3 furnishes some evidence in favor of an additional $\dot{J}$ source.

We experimented with other prescriptions for $\dot{J}$, including $\dot{J} = \dot{J}_{GR}$ with a C98 mass-radius relation, and $\dot{J} = \dot{J}_{GR}$ + *constant*. These also produce ε(P_{orb}) curves which agree with the data fairly well. Further discussion of these issues is given in Sec. 6–8 of P98.

6. SUBSTELLAR SECONDARY CANDIDATES

Ambiguity in the correct mass-radius relation on the lower main sequence is a disappointing roadblock to progress in understanding CV secondaries, and we eagerly look forward to its resolution. In the meantime, we turn to the M_2<0.07 $M_\odot$ regime.

Figure 2 shows 9 stars nominally in this regime, with M_2 below the Kumar limit (Kumar 1963; see the discussion by Henry et al. 1999, which places this at 0.076±0.005 $M_\odot$ for a Population I composition). Detailed information on these stars is given in Table 4. Uncertainties could easily carry 3 of these stars over the Kumar limit, so these are poor candidates and listed in parentheses. The two stars nominally near 0.06 $M_\odot$ are only fair candidates. The remaining four stars, with M_2 estimated in the range 0.02–0.05 $M_\odot$, are very good candidates. This conclusion would be disturbed only by a large systematic error in ε(q), or the circumstance that ε is strongly affected by some variable unrelated to q. But the good fit in Figure 1, together with agreement of the empirical ε(q) with the simplest theory (roughly $\varepsilon \propto q$), suggests that this relation is fairly robust and furnishes good evidence for inferring substellar masses in these four binaries.

Individual properties of these stars were discussed by P98. In each case, they show no luminous component identifiable as the secondary, with the white dwarf and disk accounting — within limits of observational error — for all of the detected light. Table 4 also includes three among the He-rich CVs (“AM CVn stars”), which we list for completeness although the evolution of these objects must be very different.

Is it surprising that so many CVs (8, and probably some of the other 8 with ε<0.021) have secondaries with a mass below 0.08 $M_\odot$? No, not at all. For a single H-rich star, this is a sharp threshold between (nearly) eternal life and a one-way plunge to shrinkage and death. But a CV secondary is doomed to shed mass rapidly, and passage below the Kumar limit merely means that the rate of cooling is slightly accelerated. This is because the star falls out of thermal equilibrium somewhat earlier, and the stored energy comes increasingly to dominate the star's luminosity. How much nuclear energy is freshly generated then matters little — it might as well be zero! Subsequent evolution is driven by $\dot{J}$ and the star’s slow cooling, as calculated many times previously (Rappaport, Joss, & Webbink 1982; Howell, Rappaport, & Politano 1997; KB99).

7. M_2 AND T_2 FROM FLUX MEASUREMENTS

In principle, we could constrain M_2 with spectrophotometry of the actual *light* from the secondary. In low-$\dot{M}$ dwarf novae, the white dwarf and mass-transfer hot spot tend to show M_V in the range 10–13, which for Vega-like colors (T~10^4 K) implies that the competing light has an absolute magnitude near 10–13 for all relevant passbands (R, I, J, H, K). This is formidable competition. Figure 4 shows the absolute magnitudes of main-sequence secondaries in several passbands, using the BCAH model atmospheres. Secondaries near the Kumar limit should not be significant contributors at wavelengths shorter than the J band.

But there are a few detections in the visual-infrared, and we surveyed the existing literature on detected secondaries, previously reviewed by B98 and Smith & Dhillon (1998, hereafter SD98). Those authors primarily discussed the spectral types of the secondaries, summarized in Table 1 of SD98 and Appendix B of B98. The squares in Figure 5 illustrate how the spectral types vary with $P_{\rm orb}$, compared to the trend predicted by two candidate mass-radius relations: the BCAH relation and the empirical CV relation presented above. As expected, the empirical relation gives a lower $T_{\rm eff}$, since it gives a larger R. The secondaries appear to be too cool to agree with ZAMS stars — as found also by BK00 — but agree fairly well with the empirical relation.

Does Figure 5 constitute evidence in favor of oversized secondaries? Yes, somewhat. But the number of points in Figure 5 is small, and systematic errors in the secondary's spectral-typing are worrisome. The obvious concern is that the white dwarf and accretion disk dominate below 9000 Å, so accurate subtraction of their light is quite difficult. And longer wavelengths tend to lack strong features which enable accurate spectral-typing. Yet another worry which will be important at very short $P_{\rm orb}$ is atmospheric heating of the secondary by the white dwarf. We know that heating must occur, because in eclipsing systems we are privileged to watch the white dwarfs from an angle similar to the angle appropriate to the secondary (say 3–10 deg from the orbital plane), and at that angle the line of sight is found to be essentially clear. The secondary subtends 3% of 4π sr from the white dwarf, and probably ~⅔ of that is lost from albedo and absorption in the mid-plane of the disk. Thus we expect ~1% of $L_{\rm wd}$ to heat the secondary. For a white dwarf with R=7×10^8 cm and $T_{\rm eff}$=15000 K, this produces 2×10^{29} erg/s of heating. This amounts to 1% of the secondary's nuclear $L_{\rm bol}$ at M_2=0.20 $M_\odot$, 10% at 0.09 $M_\odot$, and 30% at 0.075 $M_\odot$ (from the BCAH tables). Thus it is only a small correction to the secondary's continuum light. But because it is in the form of UV light which is easily absorbed high in the secondary's atmosphere, it will tend to weaken the temperature gradient, which is responsible for the formation of absorption lines. Weaker lines may mimic the lines of a hotter star, yielding an erroneous spectral type. To put it more generally, lines and spectral types indicate only the temperature of the line-forming region, not necessarily that of a photosphere which characterizes a deep property of the secondary (e.g., its mass or luminosity).

These uncertainties are sufficiently great that for the near future, direct detection of the secondaries at very short $P_{\rm orb}$ and accurate measurement of $T_{\rm eff}$ will probably rest on the broad-band flux distribution, not the spectral types. In either case, the accuracy of measurement will depend on reliable subtraction of accretion-disk and white-dwarf light, so that enterprise is highly recommended.

Below the Kumar limit, the secondaries burn no H, and therefore become much fainter still. But several effects may intervene to give some chance of detection. About 10^{29} erg/s is still contributed by white dwarf heating. A similar amount might be contributed by the long-term effects of heating in classical-nova eruptions (depending on how deep that radiative heating is). And thermal imbalance in the secondary provides some extra heat also (since it remembers its thermal energy from a more glorious past). The effect of all these, combined with some pressure support from increasingly degenerate electrons, is to "prop up" the radius to be nearly constant at 0.09 $R_\odot$ (according to Figure 2, and also according to the theoretical calculation of KB99 — see their Table 2). We have estimated the evolution of these factors with time, and show the expected slowly declining brightness in K light by the dashed curve in Figure 4. The initial departures from the BCAH curve are due to the thermal imbalance, calculated by KB99; the later flattening of the dashed curve arises from heating, which declines more slowly. Even after the secondary is whittled down to 0.02 $M_\odot$, $T_{\rm eff}$ is still as high as ~1500 K, giving a likely M_K near 13. Thus we expect that these are the likely practical lower limits to the brightness of CV secondaries.

Do we observe anything like this in the good substellar candidates (the four with M_2<0.06 $M_\odot$)? Not yet; the secondaries are still unseen. But one star, WZ Sge, at least has an interesting limit available. As has been well known for 20–30 years, the secondary in WZ Sge is an extremely faint star, contributing no light yet detected at any wavelength. Even in K light, the spectra and orbital light curve are still dominated by the familiar components in blue light, namely the white dwarf, disk, and mass-transfer hot spot (Ciardi et al. 1998, Dhillon et al. 2000). This limits the secondary to less than 30% of the total K light, or K >14.6, or M_K>11.4 at the 40–45 pc distance suggested by Thorstensen's (2001) preliminary trig parallax. From Figure 4 this limit corresponds to M_2<0.075 $M_\odot$ on the main sequence, or M_2<0.06 $M_\odot$ for the evolutionary (dashed) curve. It is more meaningful to express this limit as a *temperature*, since all of these short-period stars have R_2 closely equal to 0.09 $R_\odot$; the corresponding limit is T_2<2000 K.[5]

Finally, a comparable limit has been set for the secondary of EF Eri, another star very near minimum $P_{\rm orb}$. EF Eri is a magnetic CV, which does not have a disk and therefore no superhumps. It does, however, have states of very low mass transfer, in which the flux is dominated by a more-or-less pure white dwarf. Beuermann et al. (2000) studied the flux distribution at minimum, and found a strong upper limit (approximately I>21, or M_I>16) on the secondary's light from the lack of TiO features in the spectrum. For a range of possible distances

[5] Ciardi et al. (1998) constructed a similar argument for WZ Sge, and derived T_2<1700 K. But their argument used q=0.13 and R_2=0.135 $R_\odot$, values which require M_2=0.102 $M_\odot$. That is a domain in the mass-radius plane well-populated by "ordinary" dwarf novae (see Figure 2), where the secondaries are ordinarily luminous with M_K~9.3, $T_{\rm eff}$~2800 K (BCAH). Thus it requires that the WZ Sge secondary be ordinarily massive but extraordinarily (and mysteriously) dark. We consider the correct radius to be 0.09 $R_\odot$, which yields a weaker $T_{\rm eff}$ upper limit. We also prefer a more conservative "<30%" flux limit at K, because of the above-discussed concerns about heating the secondary from above. There is no mystery; the star is dark simply because it has a very low mass and thus no nuclear energy source.

and light-to-mass conversions, Beuermann et al. derived an upper limit of M_2<0.07 $M_\odot$.

The circles in Figure 5 show upper limits on T_{eff}, arising from nondetection in infrared photometry and/or spectroscopy, for the four most interesting secondaries (WZ Sge, EG Cnc, AL Com, EF Eri; the DI UMa limit is unconstraining since the accretion disk is much too bright).

8. SUMMARY

1. A useful diagnostic of CV evolution is the $\varepsilon(P_{orb})$ diagram, because it involves only strictly observable quantities which can be measured to high precision. But physically, what matters is the mass ratio q and the effective radius R_{disk}/a in the disk which drives the superhump oscillation. So we need a prescription for relating these variables, in general not observable, to quantities which can be measured.

2. We find that prescription by comparing ε with q in the stars with independent measures of both quantities (8 CVs and 5 X-ray binaries). A simple linear relation with $\varepsilon=0.216q$ is intuitive and satisfactorily fits the data available now. Refined calibrations at the highest and lowest ε are needed, however, to improve the accuracy and reliability of this relation. More sophisticated prescriptions for $\varepsilon(q)$, which proceed more directly from disk theory, should eventually replace this one.

3. Assuming this $\varepsilon(q)$ calibration and $\langle M_1 \rangle = 0.7\ M_\odot$, we make ($M_2$, R_2) estimates and compare with the simplifying assumption that "CV secondaries are on the main sequence". This comparison, discussed in Sec. 4, is confusing. CV secondaries appear to agree with the C98 empirical mass-radius law for single stars, but are slightly larger than BCAH model stars at t=10 Gyr. Thus our study is frustrated to some extent by residual uncertainty over the true M–R relation on the lower main sequence. We adopt BCAH as the provisional standard, and in Eq. (7) give an empirical M_2–R_2 relation for CV secondaries based on superhump data.

4. For M_2<0.09 $M_\odot$, R_2 trends definitely above the main sequence in Figure 2. This is probably due to increasing thermal imbalance in the secondary as it continues to lose mass. The KB99 theoretical curve tracks the data fairly well, but would be improved by assuming an enhanced $\dot{J}$ (exceeding $\dot{J}_{GR}$ by a factor 2–3).

5. The evolution of CVs in ε– P_{orb} space is studied in Figure 3 and Section 5. The values of ε dive at short P_{orb}, signifying a transition to a different M_2–R_2 relation, arising presumably from the loss of thermal equilibrium. But it is awfully curious that all CV secondaries considered here (with P_{orb}< 4 hr) appear to lie above the ZAMS, not just the ones with obvious thermal-timescale difficulties at P_{orb}=1.3 and 3.0 hrs. It is as if all CVs were fairly close to their thermal-timescale limits, a suggestion made earlier from a different line of evidence, a study of accretion rates (P84). The observed $\varepsilon(P_{orb})$ qualitatively tracks the KB99 prediction, but an assumed enhancement of $\dot{J}$ would improve the fit.

6. Again we remind the reader that the C98 mass-radius relation would fit the superhump data

excellently, as shown in Figure 2 here and Figure 4 of P98, with $\dot{J}_{GR}$ alone. Thus the most ardent GR (and Ockham's Razor) enthusiasts should especially favor the enterprise of improving the main-sequence *M–R* relation, presumably by observation of eclipsing binaries.

7. Excluding the helium-rich secondaries, we identify 11 substellar candidates, with 4 possessing excellent credentials. Three are members of the WZ Sge class, the most infrequently erupting dwarf novae. All dwarf novae with very low ε are good candidates.

8. This appears to answer one of the questions we began with: the secondaries can become substellar with no sudden change in the CV's properties. Such stars are doubtless hard to find, since they seldom erupt and are very faint in quiescence. Nevertheless, one of them is the brightest (at *V*=7.5 in outburst) and nearest (at 40–45 pc, Thorstensen 2001) of all dwarf novae, suggesting that the class may be very populous indeed. Of course it is also possible that these low-ε WZ Sge stars are the exception, with the remnants of CV evolution being predominantly *noneruptive* variables — or even non-variables — which would require different discovery techniques.

9. We study the prospects for detecting substellar secondaries from flux measurements. In general the competition from white-dwarf and accretion-disk light is too powerful. Heating of the secondary by the white dwarf is definitely important: this will weaken absorption features, raise the continuum flux, and thereby inflict another variable on interpretation of any future detections. Still, it's a mighty worthy enterprise; with proper care in subtracting the contribution of competing light sources, infrared observations may eventually reveal some of the substellar secondaries.

10. Finally, we note that results of this type signify only a transition to a different mass-radius regime (see Figure 2), not clear evidence of “bounce” after minimum period. A bounce is the simplest interpretation of Figure 3, and is predicted by every theory of CV evolution since Paczynski (1981); but other possibilities should be considered too. Maybe short-period CVs just “fall off the cliff”, lemming-like, in the ε-P_{orb} diagram of Figure 3. Or, the apparently larger dispersion at short P_{orb} (and the lack of sharp peaks in the P_{orb} distribution) may require a “soft bounce” at a *variable* minimum period, depending on idiosyncratic factors like stellar magnetism. Or both. These issues can be greatly clarified by more ε measurements at the short-P_{orb} end. A most excellent scientific reward, since the critical equipment — a small telescope and CCD camera — can be purchased and loaded into your car on the next trip to your local shopping mall.

Thanks to David Skillman, David Harvey, Robert Fried, Tonny Vanmunster, Lasse Jensen, and Jonathan Kemp for their yeoman service in the CBA, which measured many of the apsidal superhump periods. To Adam Burrows, Todd Henry, and Chris Clemens for insightful communications. And to John Thorstensen, whose relentless radial-velocity studies have made it possible to convert these numbers to actual precession rates. Without Thorstensen's role as “Inspector Javert”, the rest of us would be truly “Les Miserables”. Thanks also to the Research Corporation, which has been key to the CBA’s survival in the funding orphanage of small-science.

REFERENCES

Arenas, J. & Mennickent, R. 1998, A&A, 337, 472.
Bailyn, C.D., Jain, R.K., Coppi, P., & Orosz, J. 1998, ApJ, 499, 367.
Baptista, R., Steiner, J.E., & Cieslinski, D. 1994, ApJ, 433, 332.
Baptista, R., Cilveira, C., Catalan, S., Horne, K., & Zilli, D. 1998, MNRAS, 300, 233.
Baraffe, I., Chabrier, G., Allard, F., & Hauschildt, P. 1998, A&A, 337, 403 (BCAH).
Baraffe, I. & Kolb, U. 2000, MNRAS, 318, 354 (BK00).
Beuermann, K., Baraffe, I., Kolb, U., & Weichhold, M. 1998, A&A, 339, 518 (B98).
Beuermann, K., Baraffe, I., & Hauschildt, P. 1999, A&A, 348, 524.
Beuermann, K., Wheatley, P., Ramsay, G., Euchner, F., & Gansicke, B.T. 2000, A&A, 354, L49.
Burrows, A., Hubbard, W.B., Saumon, D., & Lunine, J.L. 1993, ApJ, 406, 158.
Charles, P.A., Kidger, M.R., Pavlenko, E.P., Prokof'eva, V.V., & Callanan, P.J. 1991, MNRAS, 249, 567.
Chou, Y., Grindlay, J.E., & Bloser, P.F. 2001, ApJ, in press.
Ciardi, D.R., Howell, S.B., Hauschildt, P.H., & Allard, F. 1998, ApJ, 504, 450.
Clemens, J.C., Reid, I.N., Gizis, J.E., & O'Brien, M.S. 1998, ApJ, 496, 352.
Danby, J.M.A. 1992, Fundamentals of Celestial Mechanics (Richmond: Willman-Bell).
Dhillon, V.S., Littlefair, S.P., Howell, S.B., Ciardi, D.R., Harrop-Allin, M.K., & Marsh, T.R. 2000, MNRAS, 314, 826.
Faulkner, J., Flannery, B.P., & Warner, B. 1972, ApJ, 175, 79.
Fleming, T.A., Giampapa, M.S., & Schmitt, J.H.M.M. 2000, ApJ, 533, 372.
Fried, R.E., Kemp, J., Patterson, J., Skillman, D.R., Retter, A., Leibowitz, E., & Pavlenko, E. 1999, PASP, 111, 1275.
Gilliland, R. & Kemper, E. 1982, ApJ, 254, 653.
Harlaftis, E.T., Horne, K., & Filippenko, A.V. 1996, PASP, 108, 762.
Haswell, C.A., King, A.R., Murray, J.R., & Charles, P.A. 2000, MNRAS, in press.
Henry, T.J., Franz, O.G., Wasserman, L.H., Benedict, G.F., Shelus, P.J., Ianna, P.A., Kirkpatrick, J.D., & McCarthy, D.W. 1999, ApJ, 512, 864.
Hessman, F.V., Mantel, H.-H., Barwig, H., & Schoembs, R. 1992, A&A, 263, 147.
Hirose, M. & Osaki, Y. 1990, PASJ, 42, 135.
Honey, W.B., Charles, P.A., Whithurst, R., Barrett, P.E., & Smale, A.P. 1988, MNRAS, 231, 1.
Horne, K., Wood, J.H., & Stiening, R. 1991, ApJ, 378, 271.
Howell, S.B., Rappaport, S., & Politano, M. 1997, MNRAS, 287, 929.
Kato, T., Mineshige, S., & Hirata, R. 1995, PASJ, 47, 31.
Kato, T., Nogami, D., Babe, H., Matsumoto, K., Arimoto, J., Tanabe, K., & Ishikawa, K. 1996, PASJ, 48, L21.
Kato, T., Nogami, D., Masuda, S., & Baba, H. 1998, PASP, 110, 1400.
King, A.R., Frank, J., Kolb, U., & Ritter, H. 1996, ApJ, 467, 761.
Kiyota, S. & Kato, T. 1998, IBVS No. 4644.
Kolb, U. 1993, A&A, 271, 149 (K93).
Kolb, U. & Baraffe, I. 1999, MNRAS, 309, 1034 (KB99).
Krzeminski, W. & Kraft, R.P. 1964, ApJ, 140, 921.
Kumar, S.S. 1963, ApJ, 137, 1121.
Kunze, S., Speith, R., & Riffert, H. 1997, MNRAS, 289, 889.

Leggett, S.K., Allard, F., Geballe, T.R., Hauschildt, P.H., & Schweitzer, A. 2001, ApJ, submitted.
Leibowitz, E.M., Mendelson, H., Bruch, A., Duerbeck, H.W., Seitter, W., & Richter, G.A. 1994, ApJ, 421, 771.
Lubow, S.H. 1991, ApJ, 381, 268.
Lubow, S.H. 1992, ApJ, 401, 317.
McClintock, J.E. et al. 2000, IAUC No. 7412.
Mennickent, R. & Arenas, J. 1998, PASJ, 50, 333
Mennickent, R., Nogami, D., Kato, T., & Worraker, W. 1996, A&A, 315, 493;
Mennickent, R.E., Patterson, J., O'Donoghue, D., Unda, E., Harvey, D., Vanmunster, T., & Bolt, G. 1998, Ap&SS, 262, 1.
Mennickent, R.E., Matsumoto, K., & Arenas, J.. 1999, A&A, 348, 466.
Montgomery, M.M. 2001, preprint.
Morley, R., Church, M.J., Smale, A.P., & Balucinska-Church, M. 1999, MNRAS, 302, 593.
Murray, J.R. 1996, MNRAS, 279, 402.
Murray, J.R. 2000, MNRAS, 314, L1.
Nelson, L.A., Rappaport, S.A., & Joss, P.C. 1986, ApJ, 304, 231.
O'Donoghue, D. & Charles, P.A. 1996, MNRAS, 282, 191.
O'Donoghue, D., Chen, A., Marang, F., Mittaz, J.P.D., Winkler, H., & Warner, B. 1991, MNRAS, 250, 363
Osaki, Y. 1996, PASP, 108, 39.
Paczynski, B. 1981, Acta Astr., 31, 1.
Paczynski, B. & Sienkiewicz, R. 1981, ApJ, 248, L27.
Paczynski, B. & Sienkiewicz, R. 1983, ApJ, 268, 825.
Patterson, J. 1984, ApJS, 54, 443 (P84).
Patterson, J. 1998, PASP, 110, 1132 (P98).
Patterson, J. 1999, in Disk Instabilities in Close Binary Systems, ed. S. Mineshige & J.C. Wheeler (Univ. Acad. Press: Kyoto), p. 61.
Patterson, J., McGraw, J.T., Coleman, L., & Africano, J.L. 1981, ApJ, 248, 1067.
Patterson, J., Bond, H.E., Grauer, A.D., Shafter, A.W., & Mattei, J. 1993, PASP, 105, 69.
Patterson, J., Augusteijn, T., Harvey, D.A., Skillman, D.R., Abbott, T.M.C., & Thorstensen, J. 1996, PASP, 108, 748.
Patterson, J., Kemp, J., Shambrook, A., Thomas, E., Halpern, J.P., Skillman, D.R., Harvey, D.A., Vanmunster, T., Retter, A., Fried, R., Buckley, D., Nogami, D., Kato, T., & Baba, H. 1997, PASP, 109, 1100.
Patterson, J., Kemp, J., Skillman, D.R., Harvey, D.A., Shafter, A.W., Vanmunster, T., Jensen, L., Fried, R., Kiyota, S., Thorstensen, J.R., & Taylor, C.J. 1998, PASP, 110, 1290.
Patterson, J., Kemp, J., Jensen, L., Vanmunster, T., Skillman, D.R., Martin, B., Fried, R., & Thorstensen J.R. 2000a, PASP, 112, 1567.
Patterson, J. Walker, S., Kemp, J., O'Donoghue, D., Bos, M., & Stubbings, R. 2000b, PASP, 112, 625.
Patterson, J., Vanmunster, T., Skillman, D.R., Jensen, L., Stull, J., Martin, B., Cook, L.M., Kemp, J., & Knigge, C. 2000c, PASP, 112, 1584.
Provencal, J. et al. 1997, ApJ, 480, 383.
Rappaport, S.R., Joss, P.C., & Webbink, R.F. 1982, ApJ, 254, 616.

Remillard, R.A., McClintock, J.E., & Bailyn, C.D. 1992, ApJ, 399, L145.
Robinson, E.L., Zhang, E.-H., & Stover, R.J. 1986, ApJ, 305, 732.
Rolfe, D.J., Haswell, C.A., & Patterson, J. 2000, MNRAS, submitted.
Rutledge, R.E., Basri, G., Martin, E.L., & Bildsten, L. 2000, ApJ, 538, L141.
Schoembs, R. 1986, A&A, 158, 233.
Semeniuk, I. 1980, A&AS, 39,29.
Shafter, A.W. 1984, PhD thesis, Univ. Calif. at Los Angeles.
Shafter, A.W., Hessman, F.V., & Zhang, E.-H. 1988, ApJ, 327, 248.
Sherrington, M.R., Jameson, R.F., Bailey, J., & Giles, A.B. 1982, MNRAS, 200, 861.
Simpson, J.C. & Wood, M.A. 1998, ApJ, 506, 360.
Smak, J.I. 1996, Acta Astr., 46, 377.
Smak, J. 1979, Acta Astr., 29, 325.
Smak, J. 1993, Acta Astr., 43, 101.
Smale, A.P., Mukai, K., Wlliams, O.R., Jones, M.H., & Corbet, R.H.D. 1992, ApJ, 400, 330.
Smith, D.A. & Dhillon, V.S. 1998, MNRAS, 301, 767 (SD98).
Spruit, H.C. & Rutten, R.G.M. 1998, MNRAS, 299, 768.
Spruit, H.C. & Taam, R.E. 2001, ApJ, in press.
Thorstensen, J.R. 2001, priv. comm.
Thorstensen, J.R. & Taylor, C.J. 1997, PASP, 108, 1241.
Thorstensen, J.R., Patterson, J.O., Shamrbook, A., & Thomas, G. 1996, PASP, 108, 73.
Thorstensen, J.R., Ringwald, F.A., Wade, R.A., Schmidt, G.D., Norsworthy, J.E. 1991, AJ, 102, 272.
Uemura, M., Kato, T., Matsumoto, K., Yamaoka, H., Takamizawa, K., Sano, Y., Haseda, K., Cook, L.M., Buczynski, D., & Masi, G. 2000, PASJ, 52, L15.
Uemura, M. et al. 2000, PASJ, in press.
Verbunt, F. & Zwaan, C. 1981, A&A, 100, L7.
Vogt, N. & Semeniuk, I. 1980, A&A, 89, 223.
Wade, R.A. & Horne, K. 1988, ApJ, 324, 411.
Warner, B. & O'Donoghue, D. 1988, MNRAS, 233, 705.
Warner, B. 1995, Cataclysmic Variable Stars (Cambridge U. Press).
Webb, N.A., Naylor, T., Ioannou, Z., Charles, P.A., & Shahbaz, T. 2000, MNRAS, 317, 528.
Webbink, R.F. 1990, in Accretion-Powered Compact Binaries, ed. C.W. Mauche (Cambridge: Cambridge Univ.), p. 177.
Whitehurst, R. 1988, MNRAS, 232, 35.
Wood, J.H. & Horne, K.D. 1990, MNRAS, 242, 606.
Wood, J.H., Horne, K., Berriman, G., & Wade, R.A. 1989, ApJ, 341, 974.
Wood, J.H., Horne, K., & Vennes, S. 1992, ApJ, 385, 294.
Wood, M.A., Montgomery, M.M., & Simpson, J.C. 2000, ApJ, 535, L39.
Zhang, E.-H., Robinson, E.L., & Nather, R.E. 1986, ApJ, 305, 740.

TABLE 1
THE ε(*q*) CALIBRATORS

Star	ε	*q*	References
WZ Sge	0.0080(6)	0.045(20)	Spruit & Rutten 1998, Krzeminski & Kraft 1964, Patterson et al. 1981
OY Car	0.0203(15)	0.10(1)	Wood et al. 1989, 1992; Schoembs 1986
Z Cha	0.0364(9)	0.145(15)	Warner & O'Donoghue 1988, Wade & Horne 1988
IY UMa	0.0260(10)	0.13(2)	Patterson et al. 2000a
HT Cas	0.0330(30)	0.15(1)	Zhang et al. 1986, Horne et al. 1991
DV UMa	0.0343(10)	0.155(15)	Patterson et al. 2000c
V2051 Oph	0.0310(10)	0.19(3)	Baptista et al. 1998, Kiyota & Kato 1998
UU Aqr	0.0702(19)	0.30(7)	Baptista et al. 1994, this work
XTE J1118+480	0.0044	<0.05	McClintock et al. 2000, Uemura et al. 2000
V1405 Aql	0.009(1)	0.025(12)	Chou et al. 2001, Smale et al. 1992, Morley et al. 1999
QZ Vul	0.0096(13)	0.042(12)	Harlaftis et al. 1996, Charles et al. 1991
V518 Per	0.017(5)	0.11(2)	Webb et al. 2000, Kato et al. 1995
N Mus 1991	0.012(2)	0.13(4)	Remillard et al. 1992, Bailyn et al. 1998

NOTE. The last five are X-ray binaries, with weaker and more uncertain constraints on *q* and ε. This class is discussed by O'Donoghue & Charles (1996) and Haswell, Murray, & King (2000). We do not now use them as calibrators, except to note their value in roughly establishing the association of low *q* with low ε. They would be fully useful if we knew that their precession (apsidal advance) rates were determined by the same physics, and the same *q*-dependence, prevailing for dwarf novae.

TABLE 2
ADDITIONAL (P_{orb}, P_{sh}) DATA

Star	P_{orb} (d)	P_{sh} (d)	ε	References*
V803 Cen	0.018657(6)	0.01873(1)	0.0041(8)	This paper.
CP Eri	0.019690(3)	0.01986(1)	0.0087(4)	This paper, Patterson 1999
V2051 Oph	0.062427(1)	0.0644(1)	0.0316(16)	This paper, Baptista et al. 1999
BC UMa	0.06261(1)	0.06447(12)	0.0298(19)	This paper
EK TrA	0.06288(5)	0.0649(1)	0.0321(25)	Mennickent & Arenas 1998, Vogt & Semeniuk 1980
AK Cnc	0.0651(2)	0.0675(1)	0.0368(33)	Mennickent et al. 1996, Arenas & Mennickent 1998
SBS1017+533	0.0679(1)	0.06955(20)	0.0243(32)	Thorstensen 2001, this paper
IY UMa	0.073909(1)	0.07583(10)	0.0260(13)	Patterson et al. 2000a
HS Vir	0.07692(3)	0.08059(15)	0.0477(22)	Mennickent et al. 1999, Kato et al. 1998
TU Crt	0.0821(1)	0.08535(13)	0.0396(27)	Thorstensen 2000, Mennickent et al. 1998
DV UMa	0.085853(1)	0.08880(10)	0.0343(11)	Patterson et al. 2000c
NY Ser	0.0976(2)	0.1038(2)	0.0635(31)	This paper
AO Psc	0.149627(1)	0.1658(3)	0.1081(20)	This paper
UU Aqr	0.163579(1)	0.17507(9)	0.0702(7)	Baptista et al. 1994, this paper

* "This paper" refers to results being prepared for full publication.

NOTE. This is a supplement to the previous catalogue (Table 1 of P98). Comments on methods of calculation in that table, and errors, apply here too. We list only stars with ε known to within 15%.

TABLE 3
CONSTRAINTS ON M_1 IN INDIVIDUAL STARS

Star	M_1 ($M_\odot$)	References
WZ Sge	0.90±0.15	Spruit & Rutten 1998
V2051 Oph	0.78±0.06	Baptista et al. 1998
OY Car	0.82±0.05	Wood & Horne 1990
CP Pup	~1.0	(fast classical nova)
HT Cas	0.61±0.04	Horne et al. 1991
IY UMa	0.85±0.11	Patterson et al. 2000a
Z Cha	0.84±0.09	Wade & Horne 1988
DV UMa	0.92±0.14	Patterson et al. 2000c
V603 Aql	~1.0	(fast classical nova)
UU Aqr	0.67±0.14	Baptista et al. 1994

NOTE. Difficulties with K_1, K_2, and i render radial-velocity solutions usually suspect. The photometric solutions from eclipsing binaries, listed here, are likely to be much more reliable. We also state a rough constraint for two fast classical novae, since nova theory definitely associates speed class with white-dwarf mass, and we consider that association to be "reliable". The other 55 apsidal superhumpers are credited with a default value of M_1=0.7 $M_\odot$.

TABLE 4
SUBSTELLAR–SECONDARY CANDIDATES

Star	P_{orb} (d)	P_{sh} (d)	ε	$M_2/M_\odot$	Period references
(OY Car)	0.063121(<1)	0.06440(9)	0.0203(14)	0.077(9)	Wood, Horne, & Vennes 1992, Hessman et al. 1992, Wood & Horne 1990
(HV Vir)	0.05711(6)	0.05833(5)	0.0214(11)	0.072(23)	P98, Leibowitz et al. 1994
(V436 Cen)	0.0625(2)	0.06383(8)	0.0212(32)	0.071(28)	Gilliland & Kemper 1982, Semeniuk 1980
(VY Aqr)	0.06309(4)	0.06437(9)	0.0203(15)	0.067(21)	Thorstensen & Taylor 1997, Patterson et al. 1993
WX Cet	0.05829(4)	0.05936(3)	0.0183(8)	0.061(18)	Thorstensen et al. 1996, O'Donoghue et al. 1991, P98
MM Hya	0.057590(1)	0.05865(6)	0.0184(10)	0.061(18)	P98
DI UMa	0.054564(2)	0.05529(3)	0.0133(5)	0.044(11)	Fried et al. 1999
AL Com	0.0566684(1)	0.05735(3)	0.0120(7)	0.040(11)	Patterson et al. 1996, Kato et al. 1996
WZ Sge	0.0566878(<1)	0.05714(4)	0.0080(6)	0.035(13)	Patterson et al. 1981
EG Cnc	0.05997(9)	0.06037(3)	0.0067(8)	0.023(12)	Patterson et al. 1998
EF Eri	0.056266(1)	(none)	(none)	<0.07	Beuermann et al. 2000
CR Boo*	0.017029(2)	0.01722(2)	0.0110(9)	0.037(12)	Provencal et al. 1997, Patterson et al. 1997
CP Eri*	0.019690(3)	0.019862(5)	0.0087(4)	0.029(7)	This paper
V803 Cen*	0.018657(6)	0.01873(1)	0.0041(8)	0.014(9)	Patterson et al. 2000b; this paper

* Helium binary.

† This limit is based on the nondetection of light from the secondary; the light-to-mass conversion is not straightforward, but a probable limit is <0.07 $M_\odot$.

FIGURE CAPTIONS

FIGURE 1. — Boxes are empirical measures of ε and q in eight eclipsing CVs, with data taken from Table 1. Ovals are more uncertain measures of ε and q in four superhumping X-ray binaries; these serve mainly to stress that low ε implies low q generally. The fitted straight line is based only on the eclipsing CVs.

FIGURE 2. — CV secondaries in the mass-radius plane. Dots are values calculated from precession rates. Crosses are precise (M_2, R_2) values from eclipsing dwarf novae. The light line is a fit to the empirical mass-radius relation in the C98 study, while the BCAH curve is the theoretical ZAMS of Baraffe et al. (1998), extended to lower mass with the (c)old solar-abundance brown-dwarf models of Burrows et al. (1993). This extension is labeled "BD" to indicate cold brown dwarfs. The dashed KB99 curve shows theoretical departures from the extended BCAH curve as a result of increasing thermal imbalance in the secondary as it evolves towards lower mass. The dashed curves at upper right show the effects on mass-radius for two fixed mass-transfer rates (in $M_\odot$/yr), calculated by Baraffe & Kolb (2000, hereafter BK00). Actual CV secondaries of M_2>0.08 $M_\odot$ appear to follow C98 very well, but are ~10–30% larger than BCAH stars. Diamonds show explicit errors for the four stars of greatest interest, and also a typical error. [The error is dominated by the expected dispersion in M_1 (±0.16 $M_\odot$); the errors in M_2 and R_2 are highly correlated because P_{orb} specifies M_2/R_2^3 to high accuracy.]

FIGURE 3. — Empirical correlation of ε with P_{orb} for apsidal superhumpers. The bold solid curve shows the trend expected from the KB99 prescription ($\dot{J} = \dot{J}_{GR}$). The "error bar" shows the range expected for a ±20% scatter in M_1, plus the uncertainty in ε(q). The dashed curves at upper right show the effects of inflicting a constant $\dot{M}$ (in $M_\odot$/yr) on the binary; these effects are large, since the secondary is then driven far from thermal equilibrium. The light solid curve shows the effect of an enhanced $\dot{J}$ (=3 $\dot{J}_{GR}$); alternative ways of oversizing the secondary (heating, adjustment of the M–R relation) produce a similar result.

FIGURE 4. — Solid curves are mass-absolute magnitude relations for main-sequence stars (BCAH models) in several passbands, extended to zero mass by assuming a constant T_{eff}=2000 K, R_2=0.09 $R_\odot$. The dashed curve is a corrected version of the changing M_K, accounting for thermal imbalance in the secondary and heating from the white dwarf. During CV evolution, main-sequence secondaries evolve from right to left.

FIGURE 5. — The expected variation of T_{eff} with P_{orb}, for two M–R relations [upper curve, BCAH; lower curve, Eq. (7)]. Squares are observed spectral types of CV secondaries, tabulated by B98 and SD98. Circles show T_{eff} upper limits for the four H-rich secondaries of lowest mass, from nondetection in spectroscopy and/or K-band photometry. We have used the BCAH M–L relation, and a T_{eff}-spectral type calibration from B98, BCAH, and Leggett et al. (2001).

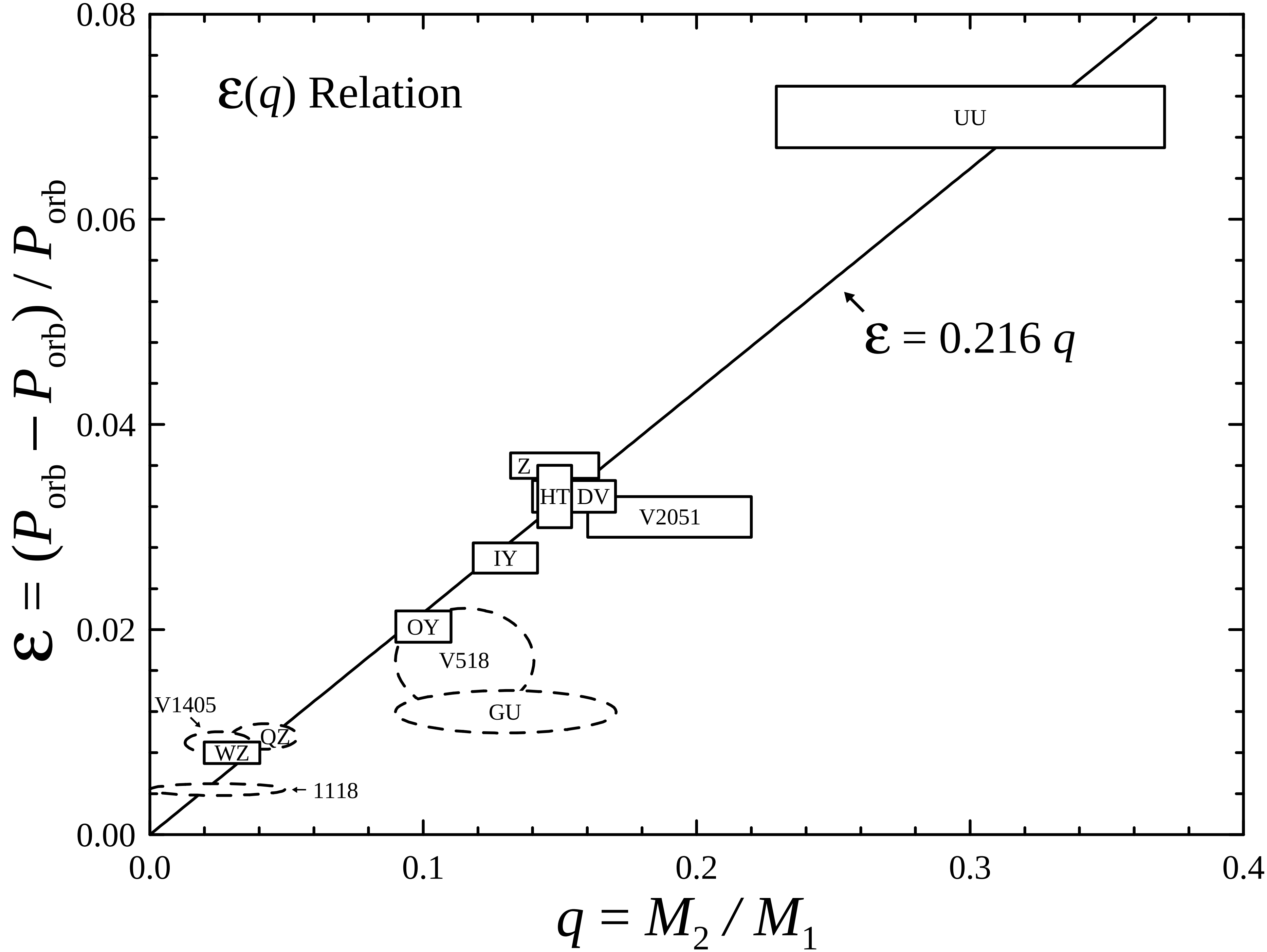

ε(q) Relation
ε = 0.216 q
UU
Z
HT
DV
V2051
IY
OY
V518
GU
V1405
QZ
WZ
1118
0.00
0.02
0.04
0.06
0.08
0.0
0.1
0.2
0.3
0.4
ε = (P_orb − P_orb) / P_orb
q = M_2 / M_1

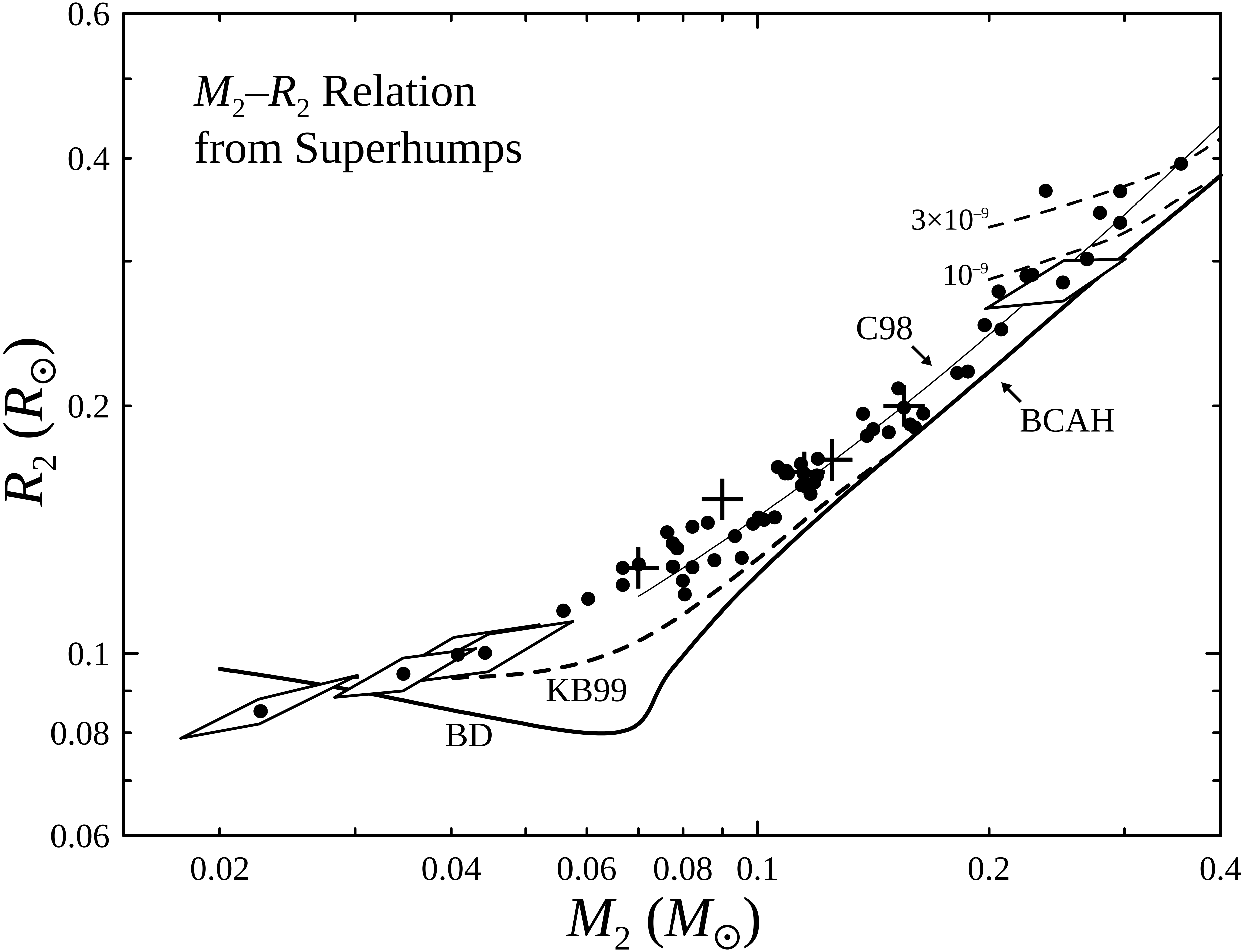
M_2–R_2 Relation
from Superhumps
3×10⁻⁹
10⁻⁹
C98
BCAH
KB99
BD
0.6
0.4
0.2
0.1
0.08
0.06
0.02
0.04
0.06
0.08
0.1
0.2
0.4
R_2 ($R_\odot$)
M_2 ($M_\odot$)

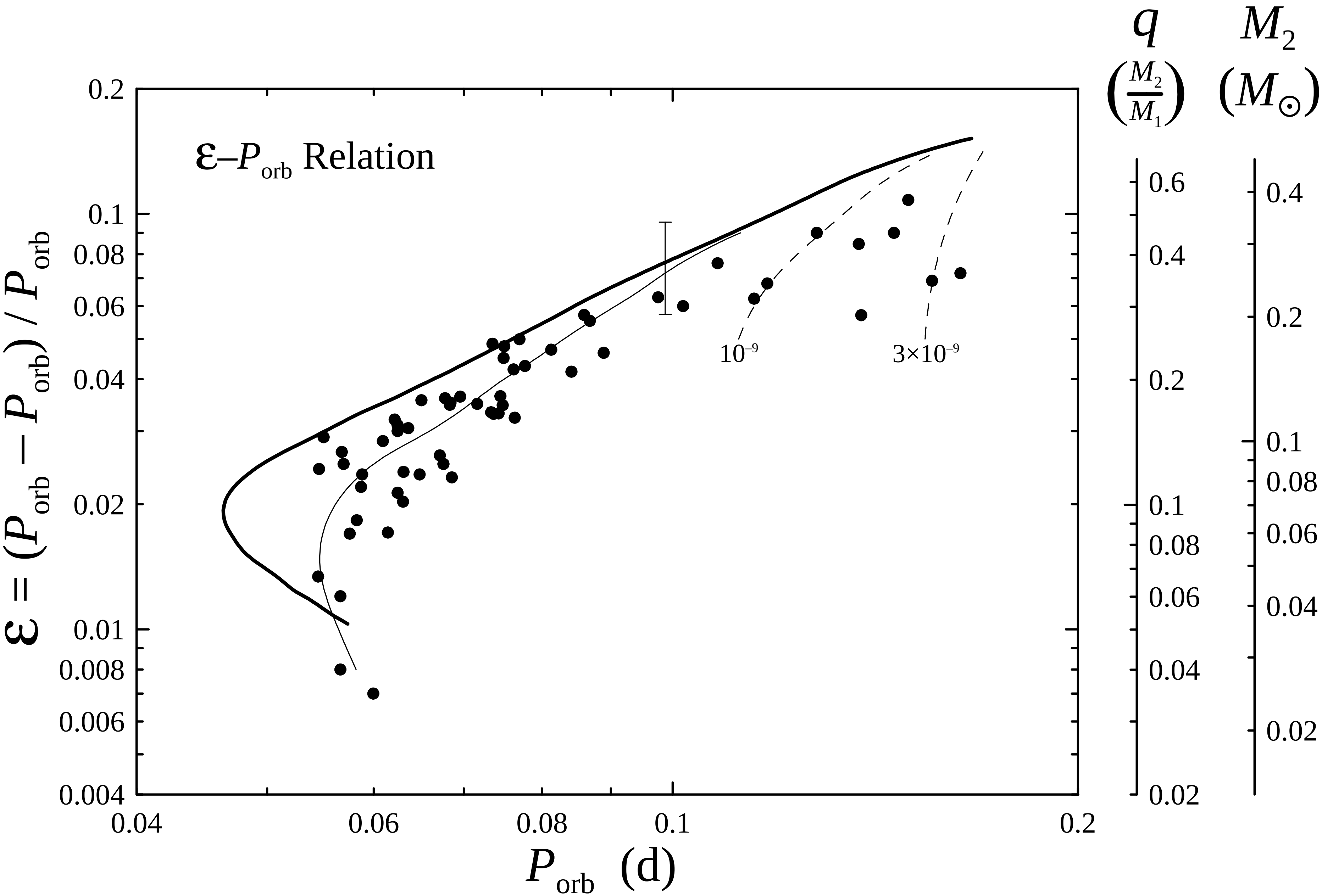

ε–P_{orb} Relation
$\varepsilon = (P_{sh} - P_{orb}) / P_{orb}$
P_{orb} (d)
q $\left(\frac{M_2}{M_1}\right)$
M_2 $(M_\odot)$
10^{-9}
3×10^{-9}
0.2
0.1
0.08
0.06
0.04
0.02
0.01
0.008
0.006
0.004
0.04
0.06
0.08
0.1
0.2
0.6
0.4
0.2
0.1
0.08
0.06
0.04
0.02
0.4
0.2
0.1
0.08
0.06
0.04
0.02

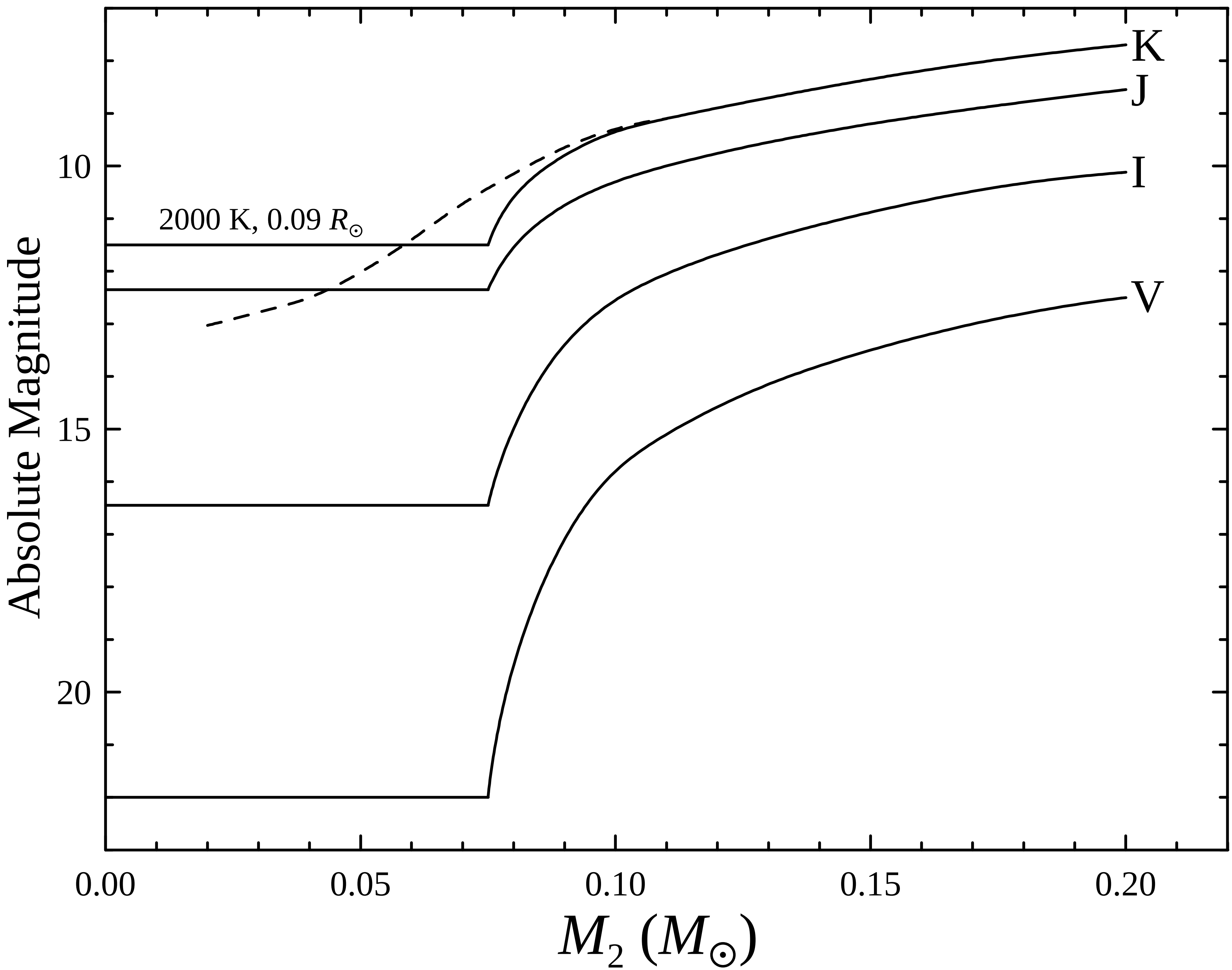
K
J
I
V
2000 K, 0.09 $R_\odot$
Absolute Magnitude
10
15
20
0.00
0.05
0.10
0.15
0.20
M_2 ($M_\odot$)

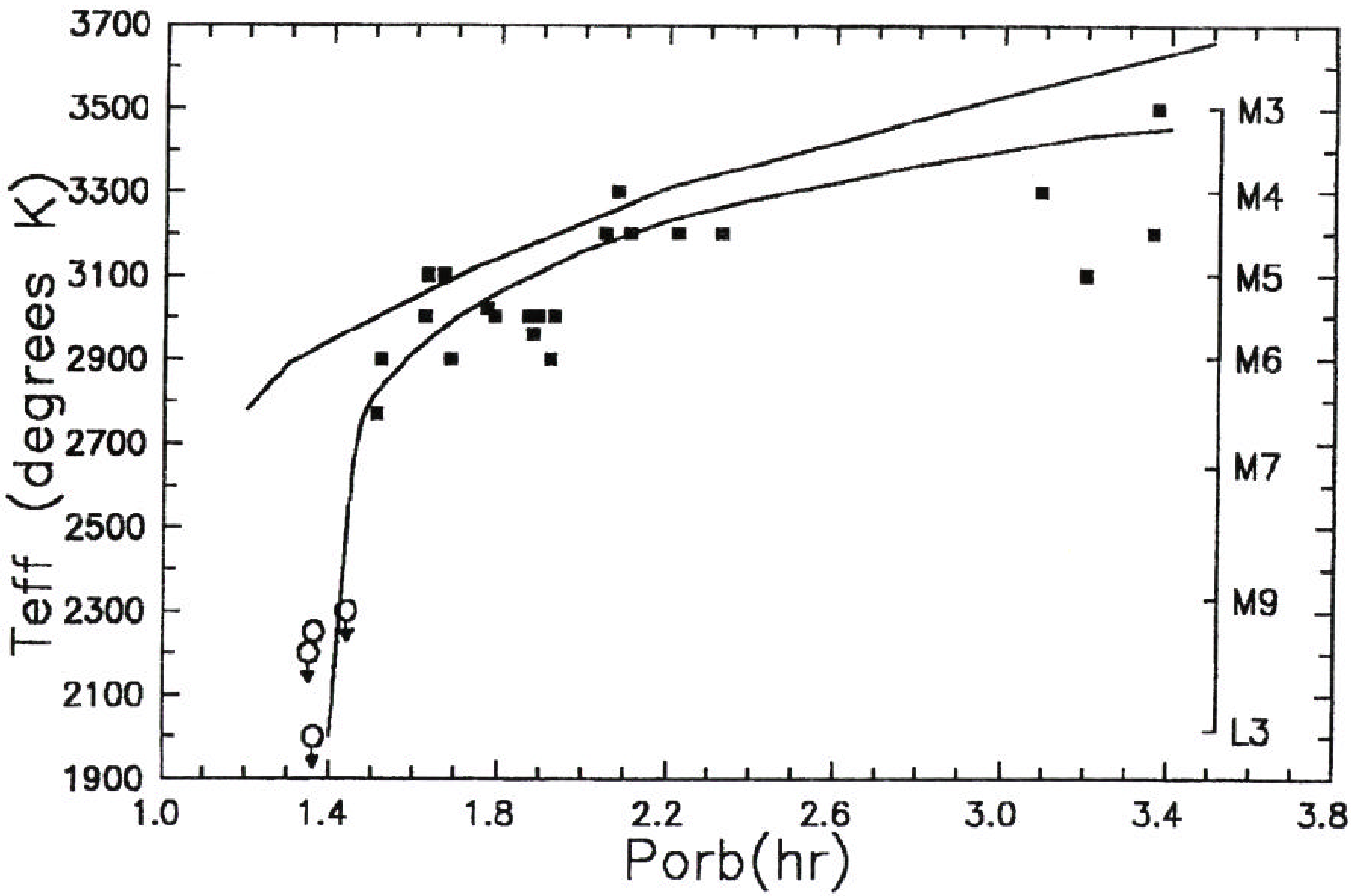
3700
3500
3300
3100
2900
2700
2500
2300
2100
1900
Teff (degrees K)
1.0
1.4
1.8
2.2
2.6
3.0
3.4
3.8
Porb(hr)
M3
M4
M5
M6
M7
M9
L3